LIMNOLOGY
and
OCEANOGRAPHY

ASLO

Limnol. Oceanogr. 61, 2016, 635–647

doi: 10.1002/lno.10240

In situ spawning in a marine broadcast spawner, the Pacific oyster *Crassostrea gigas*: Timing and environmental triggers

I. Bernard,[1,2] J.-C. Massabuau,*[3,4] P. Ciret,[3,4] M. Sow,[3,4] A. Sottolichio,[3,4] S. Pouvreau,[2] D. Tran[3,4]

[1]Ifremer, Laboratoire Environnement et Ressources des Pertuis Charentais (LERPC), La Tremblade, France
[2]Ifremer, UMR 6539 LEMAR, Site d'Argenton, Presqu'île du Vivier, Argenton, France
[3]University of Bordeaux, EPOC, UMR 5805, F-33400 Talence, France
[4]CNRS, EPOC, UMR 5805, F-33400 Talence, France

Abstract

The precise environmental conditions under which broadcast spawners spawn in the field remain largely unknown. We investigated this issue in the oyster *Crassostrea gigas* using three different methods at different time scales in two traditional oyster farming areas of the French Atlantic Coast, the Bay of Arcachon and Marennes-Oléron. We directly recorded spawning at high temporal resolution using high-frequency non-invasive (HFNI) valvometry from 2007–2014 and measured the dry mass and oyster larvae abundance in 2008 and 2009. We analyzed a 29-yr series of oyster D-larvae numbers in the Bay of Arcachon (1982–2010). By combining these three approaches, we demonstrated that during the summer months at both sites, spawning in *C. gigas* occurs in the morning or during the evening, essentially at high tide of perigean spring tides, independent of the positions of these oysters, above or below the lowest water level. We characterized the associated water currents at the spawning location in the Bay of Arcachon and observed that spawning systematically occurs during the early phase of a water current peak, at the beginning of ebbing. We propose that this water current peak acts as a final trigger for spawning. These results have ecological consequences associated with gamete encounters and the dispersal of fertilized eggs (zygotes).

For marine animals living in high-energy coastal environments, the precise timing of spawning is critical in terms of population dynamics (Levitan and Petersen 1995; Yund 2000). This critical timing is particularly true for broadcast spawners, as males and females must release their gametes into open waters where the hydrodynamic process leads to optimized encounter rates for mixing, fertilization and the dispersal of zygotes. Most studies of the reproduction of marine broadcast spawners have primarily focused on relatively long-term processes, such as gametogenesis, plankton availability (Fournier et al. 2012), larval life, spat growth, fertilization mode and evolution of life-history traits (Bode and Marshall 2007; Henshaw et al. 2014) or fish aggregation (Claydon 2004, 2014). Short-term events, such as spawning and fertilization time, have received less attention because the ability to assay natural spawning at high temporal resolution and under natural conditions is lacking. The main cue in the initiation of egg- or sperm-deposition, in terms of hierarchy, remains a matter of debate (Yund 2000), although it is associated with lunar cycles and tidal activity (Bentley et al. 2001). A wide range of triggers for spawning have been documented (Serrão and Havenhand 2009), including temperature (Minchin 1992; Grangeré et al. 2009), phytoplankton bloom (Starr et al. 1990), tides (Pearson et al. 1998) and/or twilight spectral dynamics (Sweeney et al. 2011), but reviews of bivalves (Helm and Bourne 2004) and fish (Claydon 2004) remain equivocal as to the triggers that act in the field.

Discussions concerning the underlying mechanisms that initiate spawning in bivalves date back to the beginning of the last century when spawning was reported to occur with rising water temperatures, T_w (Nelson 1928; Fujiya 1970; Arakawa 1990). A threshold temperature is necessary but not sufficient to trigger spawning in *Crassostrea virginica* according to Nelson (1928), who observed that once a basal T_w of 20°C is reached, spawning follows temperature pulses of at least 2°C in a relatively short time. Nelson (1928) and Prytherch (1929) for *C. virginica* and Hopkins (1936) for *Crassostrea lurida* observed that spawning is initiated by an adequate high-tide temperature, although water is often warmer at low tide, an event frequently observed in coastal bays during the summer. Oyster farmers are well aware that any abrupt temperature pulse of 5–10°C induces spawning in ripe oysters (Helm and Bourne 2004), and Galtsoff (1930,

*Correspondence: jean-charles.massabuau@u-bordeaux.fr

1938b) reported that male and female oysters can be induced to spawn by increasing the water temperature. Galtsoff (1930, 1938b) also reported that spawning in females can be induced in the presence of sperm. Rice et al. (2002) proposed an intrinsic membrane protein as the likely sperm pheromone in *C. virginica*, although peptides implicated in the regulatory pathway of ovulation can also trigger rhythmic contractions of the adductor muscle leading to spawning (Bernay et al. 2006). Loosanoff and Nomejko (1951) dismissed the influence of interactions between temperature, lunar cycle and spawning, although Korringa (1947) indicated that *Crassostrea edulis* most frequently spawned during spring tides, at 2 d after the full and new moons. Nelson (1928) reported that spawning occurs during or shortly after the flood tide, and Prytherch (1929) added that this event occurred near or at the time of high water (HW) during spring tides. Moreover, a relationship between spawning and spring tides was also observed by Hopkins (1936) for *C. lurida* and His (1976) and Arakawa (1990) for *Crassostrea gigas*. More recently, the comparison between diverse broadcast spawners has prompted new attempts at generalization and different conclusions. A basic observation is that fertilization success decreases with velocity and downstream distance and requires a certain level of turbulence (Quinn and Ackerman 2011). Based on mathematical modeling (Denny and Shibata 1989) and studies on sea urchin (Lamare and Stewart 1998), rockpool anemone (Marshall et al. 2004) and flucoid algae (Pearson et al. 1998), Quinn and Ackerman (2012) reported that environmentally mediated behavioral/physiological responses have evolved to reduce sperm limitations by matching spawning to favorable events, such as low tide. Clearly, several issues remain unresolved.

The objective of this study was to perform an in situ study of spawning behavior in Pacific oysters, *C. gigas*, inhabiting two ecologically different locations on the French Atlantic coast: the Marennes-Oléron basin and the Bay of Arcachon. These two sites are also traditional oyster-farming areas. Three methods were used to characterize spawning: analysis of time series of high-frequency non-invasive (HFNI) valvometry, changes in fresh oyster body mass before and after spawning and oyster larval abundance in the water column. HFNI valvometry is a new-generation remote technique enabling the online study of the behavior of bivalve mollusks living freely in their natural habitat. HFNI valvometry facilitates the autonomous long-term recordings (>1 yr) of valve movements at high frequency (10 Hz) without interfering with normal behavior (Schwartzmann et al. 2011; Sow et al. 2011; Tran et al. 2011) and without in situ human intervention. Female *C. gigas* exhibit a typical pattern of valve movement comprising a burst of rhythmic valve closures, which males do not show; males exhibit a smooth decrease in valve opening amplitude (e.g., Nelson 1928; Galtsoff 1930, 1938a; His 1976).

We demonstrated that during the summer, independent of the location relative to the water level, spawning in *C. gigas* occurred in the morning or evening, during the high tide of perigean spring tides, a period when the earth-moon distance is the shortest. At one location, we observed that spawning occurred at the beginning of ebbing, during the early phase of a water current peak.

Material and methods

Animals and high-frequency noninvasive (HFNI) valvometry

All analyses were performed using 18-month-old Pacific oysters, *C. gigas*, purchased from local oyster farmers in both sites. The in situ behavior of these organisms was recorded using a technique described by Tran et al. (2003). Briefly, light electromagnets were glued on the two shells to obtain 24/7 measurements of the amount of shell opening and closing without experimental constraints. The oysters were retrieved from the water the day before electromagnet attachment (Fig. 1A). The oysters were fixed on a piece of Netlon net (mesh size, 1.5 cm; Fig. 1E) using nylon lines to maintain a minimum distance between each specimen and placed in traditional oyster mesh bags (Netlon, 1 × 0.5 m; mesh size, 1.5 cm). The oysters were returned to the field at least 1 month prior to the beginning of the spawning period in Marennes-Oléron Bay (Banc d'Agnas, latitude 45.87°, longitude −1.17°; Fig. 1C,D). The oyster bags were fixed on an oyster table ≈0.4 m above the seafloor at a minimum water depth of ≈1 m (maximum ≈5 m during perigean spring tides). The standardization of the oyster bag area and oyster positioning facilitated comparisons of timing within groups and across years and sites. In the Bay of Arcachon (Eyrac pier, latitude 44.66°, longitude −1.16°; Fig. 1C,B), the bag was secured to a concrete slab lying on the sea floor. In Arcachon, the recording was part of a continuous online recording program, and the oysters were set in the field, depending on the year, between 3 months and 11 months prior to spawning. In both locations, the bags were located in close proximity (1–10 m) to either uncultured (larvae escaped from oyster farms, Arcachon) or cultured (Marennes-Oléron) oysters.

The HFNI valvometers were used to simultaneously record the valve activity of 16 oysters. This technology is based on the measurement of voltage variations produced from the electromagnetic field between two 56 mg coils of wire. The signal was recorded using a custom acquisition card every 0.1 s. Because 16 oysters are monitored, each oyster was measured every 1.6 s. The data were automatically and continuously transmitted daily to a data processing center in the Arcachon Marine Biological Station, using cellular and internet networks. The signals are available on the Molluscan Eye website (http://molluscan-eye.epoc.u-bordeaux1.fr/index.php?rubrique=accueil&lang=en). Sow et al. (2011)

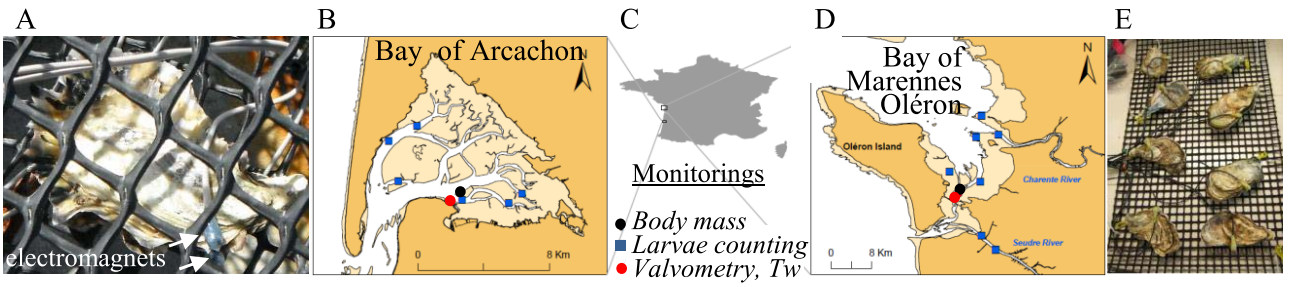

Fig. 1. (**A**–**E**): **A**, Two HFNI electrodes were fixed onto the shells of an oyster; **B**, Bay of Arcachon with the monitoring sites; **C**, location of the Bay of Arcachon and Marennes-Oléron in France; **D**, Bay of Marennes-Oléron with the monitoring sites; **E**, oysters equipped with HFNI electrodes showing the distance between the animals, and the mesh size of the Netlon net (1.5 cm). The monitoring sites are shown. T_w, water temperature. [Color figure can be viewed in the online issue, which is available at wileyonlinelibrary.com.]

showed how behavior patterns are mathematically constructed online at daily, weekly and monthly timescales. In the Bay of Marennes-Oléron, the system ran on batteries, and in the Bay of Arcachon, the system was plugged into a main power source. Two summers, 2008 and 2009, were monitored in Marennes-Oléron and five summers, 2006, 2007, 2008, 2010 and 2014, were measured in Arcachon. In both locations, only local animals were studied.

Identification of spawning events

Spawning events were identified after computing (in time periods of 15 min) the square root of the sum of squared differences of valve opening sizes, $\sqrt{\sum_i (X_i - X_{i-1})2}$, where X_i is the height of the valve opening. Spawning events correspond to maximum valve activity values, when oysters exhibit the most important valve gape activity. This method only works when there is no noise and no drift in the signal. In case of drift or noise, the search for spawning events was also performed through a visual inspection of the original valvometry records. The beginning of a female spawning event was considered as the beginning of the 1st adductor muscle contraction in a burst.

Time series of larval abundance and change of oyster body mass

To confirm and extend the spot recordings obtained by HFNI valvometry at the ecosystem level, we used two different methods: larval abundance counting and change in body mass. A historical time series of oyster D-larvae abundance was obtained from the Ifremer laboratory at Arcachon (Ifremer, Institut Français de Recherche pour l'Exploitation de la Mer), determined twice weekly from 1982 to 2002, using a constant speed plankton net trawl and from 2002 to 2010 using a seawater pumping system with a mesh size of 40 μm. Both methods provided an opportunity to evaluate the timing of the D-larvae peak. Under both conditions, the samples were fixed and the larvae counted by visual inspection using an optical microscope (Loosanoff et al. 1966; Hendriks et al. 2005). The species-specific ranges in the sizes of D-larvae made *C. gigas* larvae distinguishable, and no other D-larvae were observed between 70 μm and 79 μm in length. Moreover, in the present ecosystem dominated by oyster farming, the concentration of young oyster larvae in the water (up to 100,000 larvae.m^{-3}) becomes paramount. Confusion with other young D-larvae (for instance, *Teredo navalis* D-larvae) is likely at early developmental stages. Furthermore, each year at the beginning of the reproductive season, the technical staff from several French biological laboratories trained to recognize *C. gigas* larvae through the analysis of specific photographs and samples.

Body mass change

In pre-spawning *C. gigas*, up to 50% of the body weight is attributed to the gonads. Thus, spawning is associated with a dramatic change in the entire body mass. In both locations, we measured the dry-flesh body mass of adult oysters through repeated sampling in cultivated oyster populations. At each sampling, 30 oysters were randomly sampled, and the flesh was retrieved and weighed after a complete freeze-drying cycle. These populations were located at the "Tes" oyster bed in Arcachon Bay (latitude, 44.666°; longitude, −1.138°) and "Agnas" oyster bed in Marennes-Oléron Bay (latitude 45.871°, longitude −1.177°; Fig. 1). In Arcachon, the "Tes" oyster population is 2 km from the HFNI valvometry spot. The distance was 10 m in the Bay of Marennes-Oléron.

Environmental parameters and statistical tests

The tide data were provided by the SHOM (Service Hydrographique et Océanographique de la Marine) and directly measured in situ. The tidal coefficients were calculated as the ratio of the predicted water elevation to the elevation of a reference point. A coefficient of 20 represents the lowest tide, and a coefficient of 120 represents the highest tide. Two tide gauges were used. First, we used a tide gauge handled by the SHOM permanently set at the Eyrac pier, 5 m from the HFNI valvometer, which is part of the Sea Level Station Monitoring Facility (Station, Arcachon Eyrac http://www.ioc-sealevelmonitoring.org/index.php; IOC-UNESCO, http://www.ioc-unesco.org; sampling frequency: 1·min^{-1}). The predicted data were evaluated against

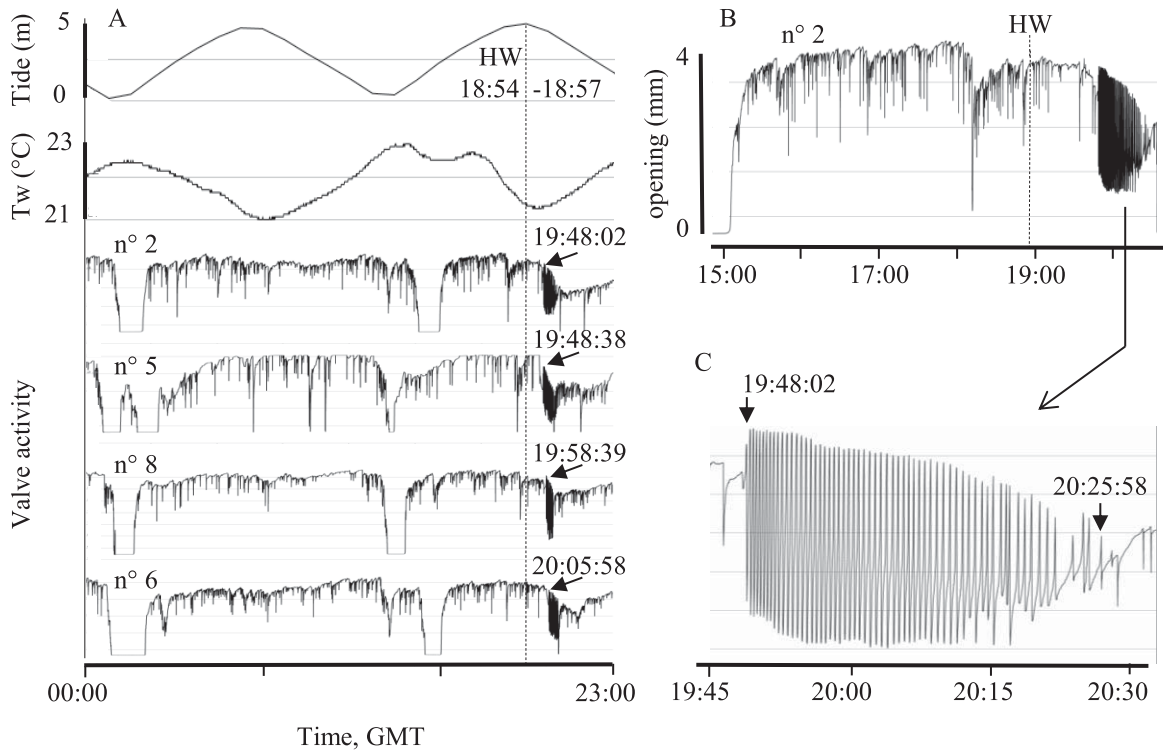

Fig. 2. (**A**–**C**): In situ recordings of typical female spawning events using HFNI valvometry, Eyrac pier, Bay of Arcachon, 15 July 2014. **A**, from top to bottom, water level, water temperature, T_w and daily activity records in four female oysters. The initiation of spawning is indicated with arrows and timed. **B** and **C**, Enlarged views at different time scales of the spawning record in oyster n° 2. Vertical dashed line in **A** and **B**, time of high water (HW). The record illustrates the maximum synchrony observed between individuals and a typical pattern of valve contraction during egg deposition. Oysters set in place on 13 February 2014.

the directly measured values. Second, the water level and current velocity were directly measured above the oyster bag using an ADV Vector 1 MHz (Nortek). The current meter was firmly fixed using a strong metal stirrup on a pile under the Eyrac pier, ≈0.2 m above the bag. This gauge was used to acquire data as close to the bag as possible (≈5 cm). Every hour, 10 min of water current and hydrostatic pressure data were recorded. Because numerous stresses or stimuli could induce artifactual spawning in ripe Pacific oysters, the battery life of the gauges limits the maximum recording duration, and setting the current meter required scuba divers to work at 0.2 m above the oyster bags, we chose to characterize the water currents on the oyster bags not during spawning but before and after spawning. We selected two contrasting periods to cover a large range of water currents: March and September equinoxes, 11 March 2007 to 22 March 2007 and 18 September 2007 to 26 September 2007. Data on the proportion of the illuminated moon and the anomalistic month of the moon were provided by the IMCCE (Institut de Mécanique Céleste et de Calcul des Ephémérides, France). The water temperature, T_w, was recorded using data loggers NKE S2T600 attached to the oyster bags and a homemade thermometer embedded in the HFNI valvometer. All data were computed and analyzed using R software (R Development Core Team 2011), with the additional package signal. The differences between distributions were assessed using the two-sample Kolmogorov–Smirnov test, with the appropriate direction (lesser or greater). The values are presented as the mean ± 1 standard deviation (SD).

Results

Characteristics of the spawning signal and timing

A total of 39 spawning events typical of egg release were recorded by HFNI valvometry. Among these, 26 events were recorded in the Bay of Arcachon (5 in 2006, 8 in 2007, 2 in 2008, 7 in 2010, and 4 in 2014), and 13 events were recorded in the Bay of Marennes-Oléron (6 in 2008 and 7 in 2009). Examples of spawning signals are presented in Fig. 2A–C, and these findings are characteristic of those already observed in female Pacific oysters and are easily differentiated from the remaining signal to noise. Briefly, the spawning signal comprised the rapid and ample movements of the valves, i.e., rapid contractions of the adductor muscle. The entire spawning event lasted 31 ± 8 min. In a burst, 51 ± 9.5 contractions occurred, and the mean period between contractions was 19 ± 6.6 s. In Fig. 2A, spawning occurred at the beginning of ebbing, 54–71 min after high tide (HW), which was a frequently observed delay (see below). Notably, spawning occurred when the T_w was at a

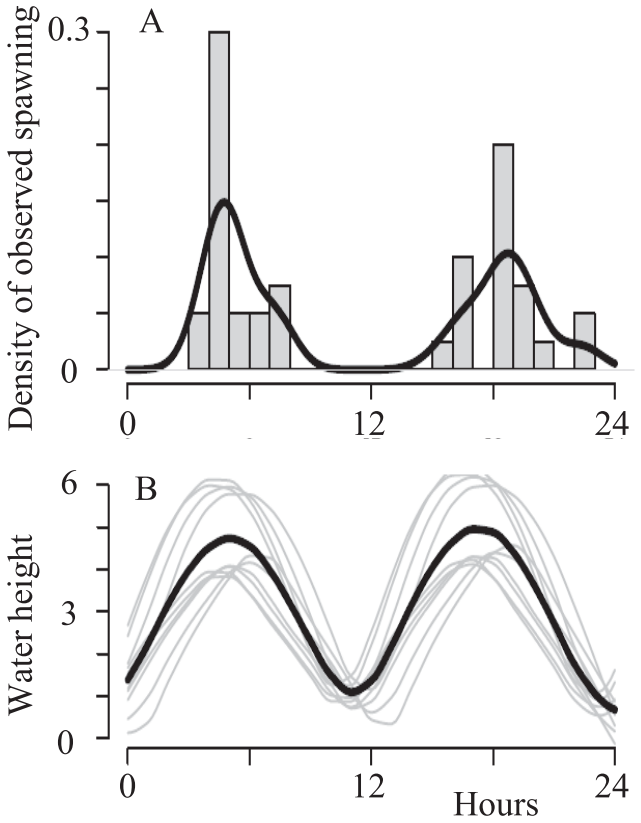

Fig. 3. (**A**, **B**): **A**, Daily distribution of all recorded timings of female spawnings (spawning starts; GMT; Bay of Arcachon and Marennes-Oléron) with the corresponding density curve. **B**, The water height cycles on the days spawning was observed (pale gray), ignoring year and studied site, are drawn from the hourly height of the water using piecewise cubic hermite interpolation. The black curve shows the piecewise cubic hermite interpolation of all hourly data for the water heights used. Spawning occurs each year at high water levels in early morning and late afternoon.

minimum in the temperature oscillation characteristic of the Bay of Arcachon during this season and salinity at the maximum annual value (32–34‰). Figure 2B,C are enlarged views showing the details of *C. gigas* behavior prior to and during spawning and the delay between high tide and spawning (taken from oyster n° 2 in Fig. 2A). Figure 2A also illustrates the synchronization observed among individuals. Importantly, this synchronization was variable from year to year and between sites, although the oysters were consistently maintained in oyster bags with a standardized surface area of 0.5 m^2. In only three of the seven cases, we recorded a single sequence of spawning, as observed in Fig. 2A. In these cases, the minimum delays between the first and the last spawning events were 23 min and 17 min (Arcachon; $n = 8/16$ and 4/8; female spawning/total number of oysters) and 74 min (Marennes-Oléron; $n = 7/16$). In all other cases (4/7 cases), despite similar experimental conditions, and for the same proportion of spawning females in the bags, the total sequence took 2–3 d. In most but not all oysters that did not exhibit the typical egg release behavior shown in Fig. 2, we observed a regular decrease in the valve amplitude typical of sperm release. Contrary to egg release, the precise beginnings and endings were impossible to characterize by comparison to a reference pattern, but to the best of our knowledge, this behavior lasted approximately 2–5 h.

At what time of the day did the oysters spawn?

Independent of the site and year, a clear pattern emerged (Fig. 3A). Spawning occurred either in the morning, most frequently from 4 h to 8 h GMT, or in the evening, from 16 h to 20 h GMT. Spawning never occurred around noon or at midnight. Thus, spawning time was not randomly distributed around the clock. When the water level for each of these days was included (Fig. 3B), a highly similar set of distribution curves was obtained. Clearly, spawning occurred each year at high water levels during early morning and late afternoon.

Spawning triggers

Based on previous studies (*see* Introduction) and the data obtained in this study, the initial spawning triggers were tide and lunar phase, as high tides of spring consistently occur around sunrise and sunset at both bays examined. We thus asked the following questions: Is there a difference between sites? At what point in the high tide is spawning most frequently initiated? Is there a minimal tidal coefficient above which oyster spawning occurs? Is spawning associated with a particular lunar phase and cycle? Figure 4 presents the relationship between these various environmental triggers, their natural distributions and the onset of individual spawning events.

Differences between sites

Figure 4A1 (Marennes Oléron) and 4A2 (Arcachon) present spawning frequency distributions, considering the time of high water as t_0 (vertical dashed line, HW). Obviously, the distributions were not similar. At Marennes-Oléron, spawning was largely distributed from −113 min to +92 min before and after high water. Three groups were tentatively defined in Fig. 4A1: 54% of spawning occurs around the slack water of high tide (−56 to +21 min), 8% of spawning occurs at the end of rising tide (−113 min) and 38% of spawning occurs at the beginning of ebbing (+54 to +79 min). Alternatively, under the Eyrac pier in Arcachon, the distribution was much narrower, and 100% of the female oysters spawned from 48 min to 120 min after high water, i.e., at the beginning of ebbing. Figure 4B also shows that all spawning at Marennes-Oléron was specifically associated with a high tide coefficient ranging from 98 to 102, while under the Eyrac pier, the coefficient range was lower, ranging from 69 to 98.

We next examined the role of the lunar phase based on the percentage of illuminated moon. Figure 4C shows that

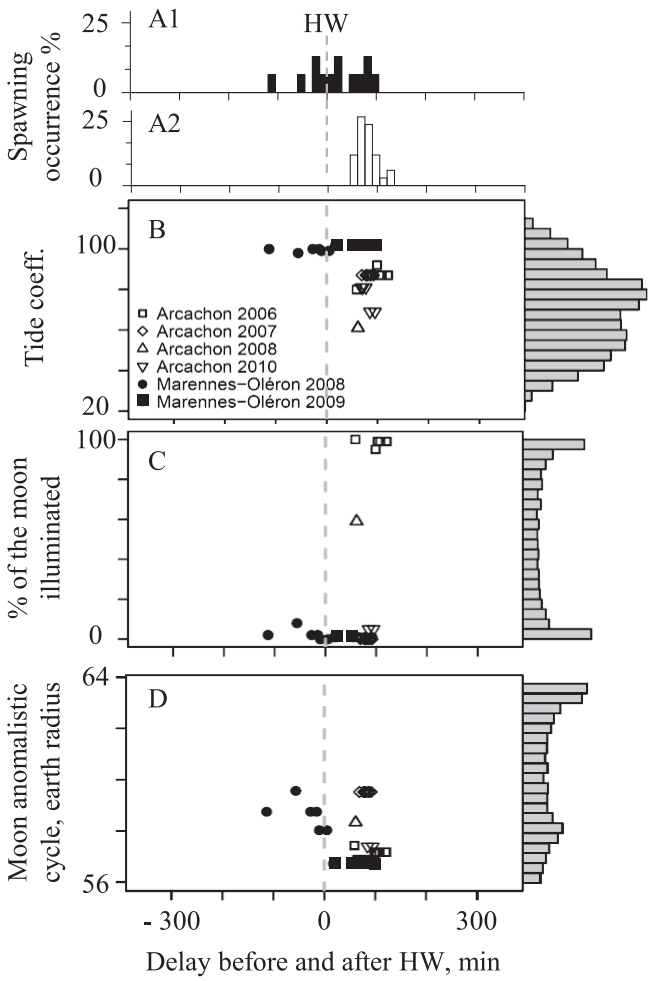

Fig. 4. (**A1**, **A2**, **B**, **C**, **D**): Distribution of all recorded female spawning initiated as a function of time before or after high water level (HW) and other environmental factors. The vertical dashed line is t_0, the time of high water, HW. **A1**, distribution in Marennes-Oléron; **A2**, distribution in the Bay of Arcachon; **B**, relationship between tide coefficient; **C**, percentage of the moon illuminated; and **D**, moon anomalistic cycle expressed in number of earth radii as a function of time and delay before or after HW. The probability distributions of the summer value (July–August) of these three parameters are drawn in the right margin (gray histograms). See text for explanations.

in 80% of cases, spawning occurred at the new moon ($n = 32/40$), while in 15% of cases, spawning occurred at the full moon ($n = 6/40$) and in 5% of cases, spawning occurred at an intermediate moon phase ($n = 2/40$; last quarter moon phase). Figure 4C also shows that in Marennes-Oléron, all spawning occurred at the new moon, while in the Bay of Arcachon, spawning occurred, in all but two instances, either at the full or new moon. We next focused our attention on another indirect indicator of tide amplitude, the distance between the earth and moon, referred to as the anomalistic month of the moon (Fig. 4D), which varies according to a cycle of 27.55 d. Under a semi-diurnal tidal regime, when this distance is large, a lower spring tide is generated during the full or new moon. A short distance, however, reinforces the effect of the lunar phase on tide amplitude. Figure 4D clearly shows that the entire set of spawning events detected through HFNI valvometry occurred when the earth-moon distance was the lowest, unmasking a powerful influence.

What about the temperature effect?

Temperature and heat shocks are well known triggers of spawning in mollusk hatcheries. Specifically, a sharp temperature change (+5–10°C within 1 h or abruptly) is often used to trigger spawning in cupped (Pacific) oysters. The timing of spawning during the T_w cycles in the Bay of Arcachon is illustrated in Fig. 2, and here, we show the mean T_w measured during the 24-h period preceding all recorded spawning and the corresponding values of $T_{w\ max} - T_{w\ min}$ for that precise 24-h period (Fig. 5A, Arcachon; Fig. 5B, Marennes-Oléron). Distributions describing the natural T_w range in July–August are drawn in the margins for comparative purposes. Figure 5A,B show that spawning occurs when T_w ranges from 20°C to 24.2°C and $T_{w\ max} - T_{w\ min}$ ranges from 1.4°C to 4.1°C, the upper range of the summer distributions. Notably, only 2 out of 40 (5%) spawning events were associated with a thermal amplitude of water of 1.4°C in the 24 h prior to spawning. The mean temperature distribution was narrower in Marennes-Oléron (20.4–20.6°C) than in Arcachon (20.9–24.2°C).

Why was the spawning period so narrow in Arcachon and why do oysters spawn 80–120 min after high tide?

To obtain more insight into this question, we analyzed the current velocities at the oyster bag site in Arcachon. The results are presented in Fig. 6. Figure 6A shows a global view of the current velocities from neap tides to spring tides in March 2007. Figure 6B1,B2 are enlarged views of two spring tides, showing that above the oyster bag, at the very beginning of ebbing (vertical dashed lines), the water velocity dramatically increased from less than 0.1 to ≈0.5 $m \cdot s^{-1}$ within 1 h. Subsequently, the water velocity remained elevated for 2–2.5 h prior to gradually slowing down. The pattern was similar in September (data not shown), demonstrating that when the flow velocity peaked, all oyster spawning at this site was recorded (inserted histograms redrawn from Fig. 4A2). Moreover, Fig. 6C shows the global relationship between the maximum current velocity and tide coefficient for all water current measurements. The vertical dashed lines here delimit the range of tide coefficients associated with spawning, showing that oyster spawning at Eyrac was associated with maximum water velocities of 0.45–0.60 $m \cdot s^{-1}$.

Studying spawning on a larger scale in Arcachon and Marennes-Oléron

The above dataset was obtained with high precision timing at small spatial scale (0.5 m^2). To characterize its representativeness at a larger scale, the data obtained with the

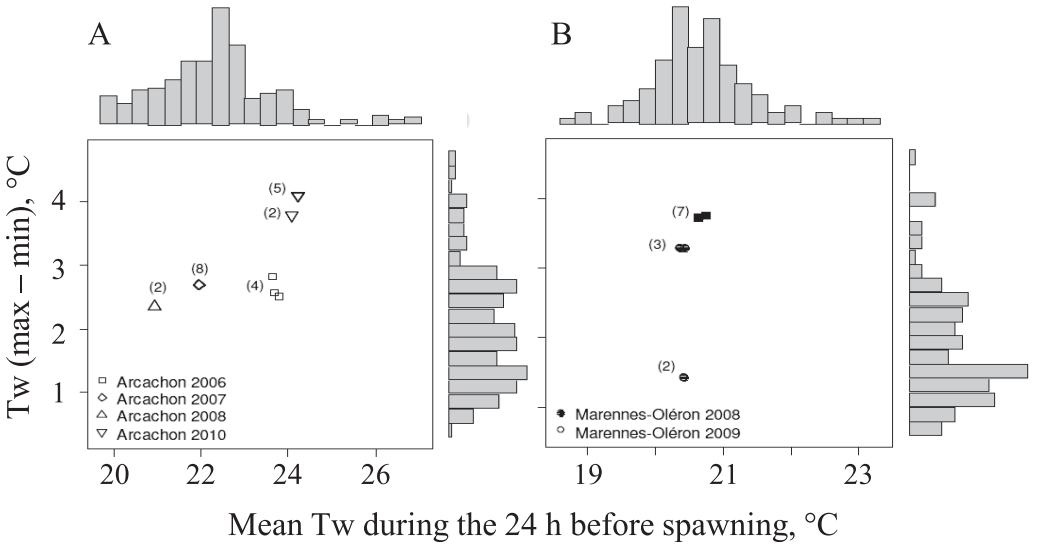

Fig. 5. (**A**, **B**): The mean sea temperature, T_w, and maximal temperature amplitude of water (max−min) at 24 h prior to spawning for every recorded spawning event in Arcachon Bay (**A**) and Marennes-Oléron Bay (**B**). The summer distributions of the mean temperature and temperature amplitude of the water for the studied years are drawn in the upper and right margins. The numbers in brackets indicate the number of observed spawning oysters for each spawning event, represented by different symbols.

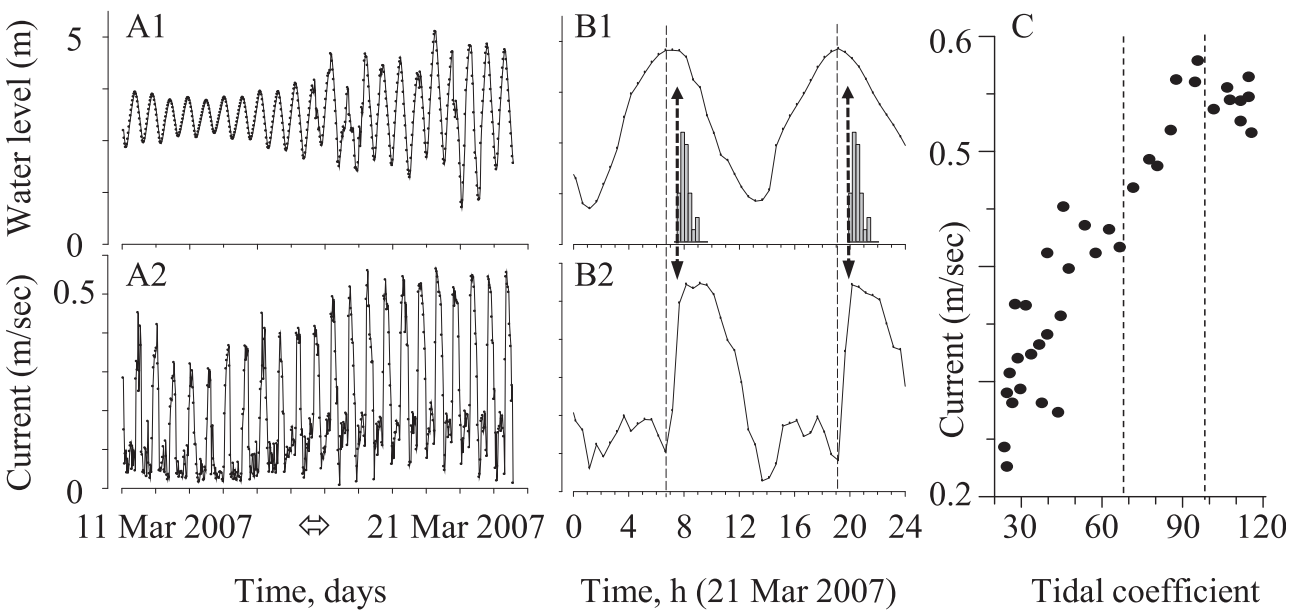

Fig. 6. (**A1**, **A2**, **B1**, **B2**, **C**): Characterization of water flow on the oyster bag where all spawnings were recorded under the Eyrac pier in the Bay of Arcachon. **A1** and **A2**, simultaneous recordings of water level and water current during the period 11 March 2007 to 21 March 2007. **B1** and **B2**, enlarged view of the records on 21 March 2007. Insert in **B1**, distribution of female spawning starts at Eyrac (redrawn from Fig. 4A2) with t_0, the time of high water level. Only one water current peak was observed at this site, during ebbing, and all spawning began during the early part of this peak. **C**, relationship between maximum water current velocities and tide coefficients at Eyrac. All spawnings were recorded at tide coefficients ranging from 69 to 98 (vertical dashed lines).

HFNI valvometers were compared with two other independent proxies of oyster reproductive cycles: (1) the difference in individual dry-flesh body mass before and after spawning and (2) oyster D-larvae concentrations in the water column. Figure 7 shows the results for the Bay of Marennes-Oléron in 2008 and 2009. The spawning events recorded by HFNI valvometry are presented as the vertical bar. In 2008 (Fig. 7A), the spawning recorded by valvometry occurs when the dry flesh mass of nearby populations decreases and when a single peak of D-larvae abundance appears in the water column.

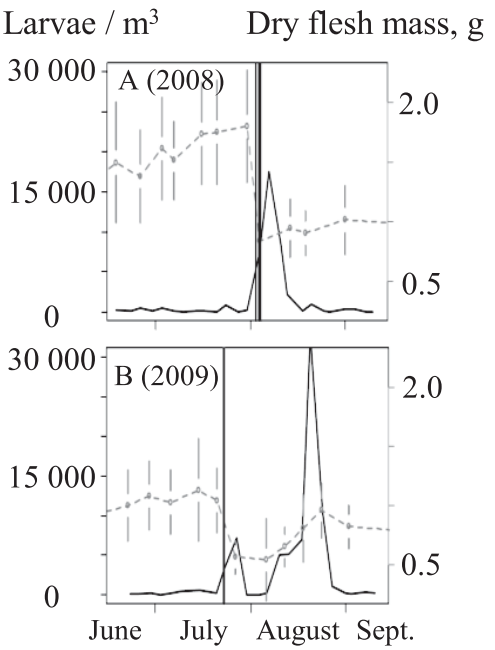

Fig. 7. (**A**, **B**): Relationship between spawning events detected using HFNI valvometry (vertical bars), showing a simultaneous decrease in dry flesh mass of nearby oyster populations (dashed gray line) and oyster larval abundance (continuous black line), at the Bay of Marennes-Oléron in 2008 (**A**) and 2009 (**B**). In 2008, the spawnings recorded using HFNI valvometry were clearly representative of massive spawning in the area. In 2009, these measurements were associated with an initial spawning event, but the main mass spawning in the Bay occurred later on.

In 2009 (Fig. 7B), the valvometer recorded a first local spawning event and the subsequent main mass spawning in the Bay. This entire dataset illustrates spawning variability at an ecosystem scale. Together with the above description of micro-scale kinetics and heterogeneity, this dataset also documents the reality of synchrony and asynchrony in broadcast spawners.

Moreover, we analyzed a long-term time series (1982–2010) of D-larvae abundance for the Bay of Arcachon. While it provided a unique method to examine the robustness of the above observations, the D-larvae abundance approach has the major drawback of not being precise, as spawning can only be inferred with an accuracy of 3 d. Indeed, when an oyster D-larvae peak is detected, a spawning event occurred 2–4 d earlier. Figure 8 presents distributions of the water thermal amplitude, tidal coefficient and moon anomalistic cycle at spawning (based on D-larvae counts) in the Bay of Arcachon. We also included the thermal amplitude in air during the days prior to spawning, as oysters living in the intertidal zone are directly exposed. For each of these parameters, two distributions were drawn. The continuous line represents the random distribution of the studied parameter in July–August 1982–2010 (61 d/yr), and the dashed line represents the recorded distribution occurring 3 d prior to the peak of oyster D-larvae. A perfect fit between the curves suggests the absence of a relationship with the studied environmental parameter. In contrast, a difference between the curves suggests that spawning only occurred on particular days. For daily air temperature, a clear difference was observed between the random distribution and the distribution of thermal amplitude prior to spawning (Fig. 8A). High air temperature amplitude, above 12°C, was associated with

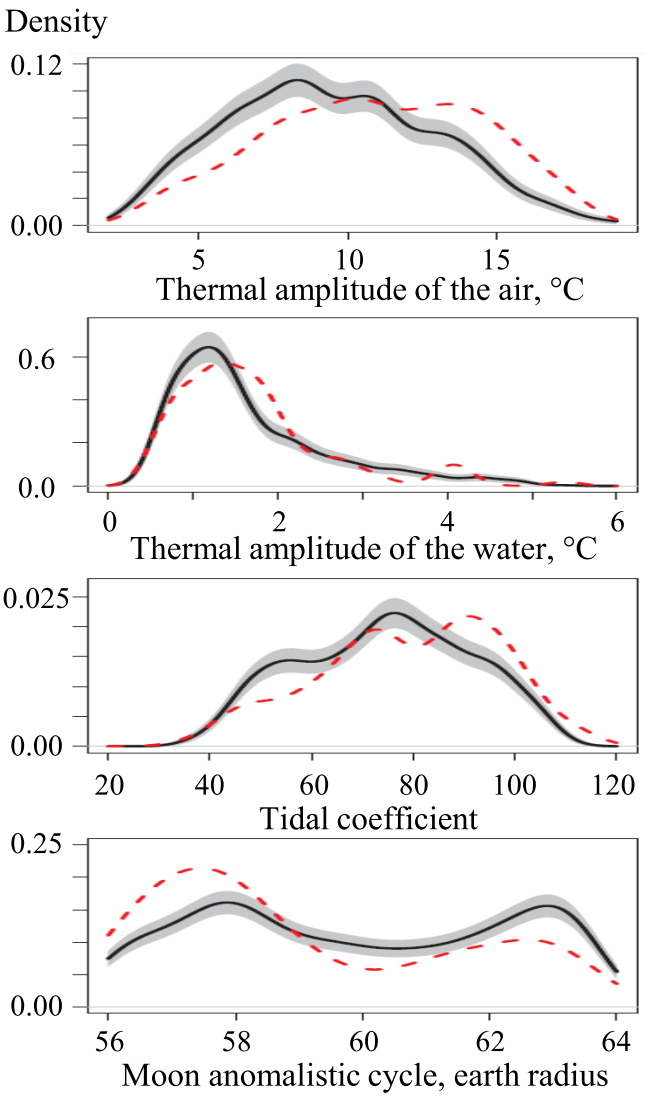

Fig. 8. (**A**–**D**): Large scale analysis (29 yr from 1982 to 2010) of the relationship between spawning and selected environmental factors in the Bay of Arcachon. Probability density of temperature amplitude of the air (**A**), temperature amplitude of the water (**B**), tidal coefficient (**C**) and anomalistic cycle of the moon (**D**) at spawning time (dashed line) compared with the summer distribution of these parameters (continuous line). The gray surfaces represent the 95% confidence intervals of the estimation of summer distributions. Spawning time is defined as the period from 2 d to 4 d before D-larvae peak, and the maximal parameters during this 3 d period are shown. High daily temperature, tide coefficient above 69 and shortest earth-moon distance are associated with spawning in *C. gigas* during the entire period. [Color figure can be viewed in the online issue, which is available at wileyonlinelibrary.com.]

oyster spawning (two-sample Kolmogorov–Smirnov test, $p = 10^{-7}$, $n = 236$). For the temperature amplitude of the water, a low significant difference between the two distributions was observed (Fig. 8B, two-sample Kolmogorov–Smirnov test, $p = 0.042$, $N = 214$). For the tidal coefficient, spawning preferentially occurs during the high tide coefficient, above 60–70, corresponding to spring tides (Fig. 8C). Notably, an important difference between the two distributions was observed at approximately 95 (two-sample Kolmogorov–Smirnov test, $p = 8.4 \times 10^{-5}$, $N = 254$), confirming the influence of perigean spring tides. Moreover, Fig. 8D shows that during this 29-yr time series, spawning clearly occurred more frequently when the earth-moon distance was shortest (two-sample Kolmogorov–Smirnov test, $p = 3.2 \times 10^{-6}$, $N = 254$). This large dataset statistically supports the preferential occurrence of spawning of the Pacific oyster, *C. gigas*, on the French Atlantic coast during periods exhibiting large air temperature changes and at spring tides when the earth-moon distance is the shortest, i.e., during perigean spring tides.

Discussion

This report provides a precise study of the spawning strategy in a broadcast spawner studied in the field under natural conditions. This study focused on the Pacific oyster *C. gigas* in two field locations along the French Atlantic coast where oysters spawn from early June to mid-September (His 1976), when water temperature and salinity are close to the maximum annual value. We studied a permanently immersed location (in the Bay of Arcachon) and an intertidal zone (in the Bay of Marennes-Oléron) and demonstrated that spawning systematically occurred at high tide of perigean spring tides. At one site, spawning systematically occurred 80–120 min after high tide, and taking advantage of this phenomenon, we showed that spawning at this site was synchronized to the beginning of a water current peak associated with the ebbing tide. In the hierarchy of spawning cues existing in *C. gigas*, we propose that this water current peak acted as a final spawning trigger. Spawning was more frequent during the new and full moon and during the lunar perigee and was never observed at a tidal coefficient lower than 69. Spawning systematically occurred during the day, around either sunset or sunrise. As high tides in the spring occur at sunset and sunrise in the studied areas, these data did not discriminate between tides and changes in sunlight, but the direct influence of moonlight can be excluded. Days with large thermal amplitudes were a positive factor, although the initiation of spawning was not associated with maximum temperatures, as during this season, the maximum T_w is at low tide. The minimum water temperature change in the 24 h prior to spawning was most frequently 2.5°C.

In multiple species of reef fishes, Claydon et al. (2014) reported that the majority of fish spawned during the days around the new moon, with higher tides, at sunrise and before sunset. Also in most crustaceans, crabs release larvae during maximum-amplitude high tides, often during early ebbing (Morgan and Christy 1995). Thus, present observations fit well with some of the known spawning strategies, although species-specific differences do occur.

It was not possible to determine whether male or female spawning is initiated on the release of egg and/or sperm in a orderly manner. Under clam farming conditions, Helm and Bourne (2004) reported that, "it is generally the case that males will spawn first but this cannot be guaranteed." The global synchronization of in situ spawning also appeared much more irregularly than expected at small spatial scale (0.5 m^2), as close female individuals can spawn at the same time each day but at 1–3 d intervals. This observation is contrary to the traditional view of spawning as a highly synchronous event (Galtsoff 1961) but consistent with other species considered synchronous: 3 d for the worm *Palolo viridis* (Caspers 1984), three successive low tides for the ascidian *Pyura stolonifera* (Marshall 2002) or two to four successive days for the sea cucumber *Isostichopus fuscus* (Mercier et al. 2007). Marshall (2002) also noted that, as in *C. gigas*, synchronization at the individual level is not perfect but does not impact fertilization success at the population level.

In this study, we focused on identifying spawning triggers in the field. Temperature is a well-known spawning driver in hatcheries where a thermal cycling procedure with a differential of ≈5–10°C and periods of 30–40 min is used. When the temperature is changed, a small amount of algae are added to stimulate pumping activity and subsequent soft body warming or cooling (Helm and Bourne 2004). During the summer, the animals might spawn within an hour of induction. This technique has been extensively studied and used for various edible bivalves, i.e., blue mussel *Mytilus edulis* (Pronker et al. 2008), Pacific and pearl oysters *C. gigas* and *Pinctada margaritifera* (Southgate and Beer 1997), American oyster *C. virginica* (Dupuy et al. 1977), European clam *Venerupis decussatus* (Matias et al. 2009), giant clam (Ellis 1998) and brackish water bivalve *Corbicula japonica* (Baba et al. 1999). In this field study, such changes in temperature were never observed, although for individuals in the intertidal zone, a combination of air vs. water temperature (at rising tide) could create complex thermal patterns (Helmuth et al. 2002). The air temperature at Marennes-Oléron was 24–25°C during the spawning periods, similar to the water temperature, therefore excluding the influence of a large heat shock with the first waves at rising tide. Other drivers have been implicated during spawning. Considering the moonlight effect, which has a well-known influence on Palolo worms (Caspers 1984), it is worthwhile to note that spawning occurred during the day in *C. gigas*, eliminating moonlight de facto as a key trigger for the species. In the lugworm *Arenicola marina*, spawning occurs at a particular combination of tide and weather conditions (Watson et al.

2000). The artificial presence of sperm (Rice et al. 2002), large changes in salinity (Southgate and Lee 1998) or exposure to high algae concentrations (2–2.5 million cells·mL^{-1}, Breese and Robinson 1981) also stimulate spawning under small-scale artificial conditions. None of these stimuli occurred in this study. Hydrostatic pressure and current velocity associated with perigean high tides are factors associated with spawning at high tide, although these factors have rarely been discussed in previous studies.

Why does spawning occur close to the high tide? The expulsion of gametes

In female *C. gigas*, eggs are expelled in the water column during a series of fast contractions, resulting in high pressures in the palleal cavity. The gonad comprises many-branched, ciliated ducts from which numerous sacs open. During maturation, the gonaducts carrying the gametes develop and enlarge. The gonaducts join the kidney tubule to form a common chamber, the atrium, which opens into the cloaca. When the gonads are fully mature, the gonad size is greatly increased, and in *C. gigas*, the gonads represent half of the entire soft tissue mass, while the inner space in the valve cavity is not proportionally changed. The resulting problem of congestion is such that in pre-spawners, the gonad volume mechanically constrains the pericardial sinus and ventricle (Pouvreau et al. 2006), limits cardiac output and brings the animals into a respiratory insufficient status (Tran et al. 2008). Thus, spawning at high tide, when the hydrostatic pressure is maximal on the gonads, suggests that any additional pressure should facilitate the expulsion of gametes. Because a water column of 1 m exerts a pressure of 100 g cm^{-2}, any increase in hydrostatic pressure can affect the gonads as long as there is no exchange of fluid or matter between the internal and external milieu. However, why does spawning occur during perigean spring tides? Indeed, in most cases, the difference in water levels between perigean spring tides, which occur 3–4 times a year, and normal spring tides, which occur twice each month, is small, ≈0.1–0.15 m (http://oceanservice.noaa.gov/facts/perigean-spring-tide.html). As shown in this study, the missing link could be water current. However, evidently, in the hierarchy of spawning cues, this event also requires the full maturation of gametes and gonads, high global T_w, temperature swings and high water levels. Thus, water current velocity at perigean spring tides might be the capstone of an entire set of factors, i.e., the last straw that drives oyster spawning.

Gamete encounters and dispersal of fertilized eggs

The timing described above has numerous ecological implications. Indeed, massive and synchronous gamete release is considered to be critical to the reproductive success of broadcast spawners with external fertilization. Spawning must be constrained within narrow windows of opportunity to maximize the probability of gamete encounters. The data obtained in this study provide evidence for and against these ideas and suggest possible modulations in gamete encounters. Indeed, this study demonstrates that simultaneous spawning for congeners living in a small area (0.5 m^2) is not the rule; in fact, in *C. gigas* this event is the exception. Thus, the local concentration of gametes is less than one would observe after synchronized massive spawning. Any conclusion is speculative, but an excessive gamete concentration could be counter-productive in some, as yet unknown, manner. More specifically, a single rather than synchronized spawning event might reduce the likelihood of fertilization between close partners and/or polyspermy (see below). In this view, one must keep in mind that 3-yr-old female *C. gigas* have up to 230 million eggs in their gonads prior to spawning (mean value, 146 million, Royer et al. 2008).

While spawning in a small group of *C. gigas* can occur on different days, for individuals spawning within a narrow time window, there is a specific moment for this event to occur. Studies have shown that at both sites, despite different conditions, *C. gigas* essentially spawns before and/or at the beginning of ebbings of high perigean tides. Under the Eyrac pier in Arcachon Bay, where spawning time was systematic in a precise, consistent and reproducible manner from year to year, we showed that spawning occurs at the onset of ebbing currents, which are more likely to reduce the temporal window for gamete encounters between spawning partners. We propose that spawning at this time should influence fertilization in two ways. On the one hand, turbulence in relation to bed roughness fundamentally influences the probability of encounters, impacting both gamete dilutions and egg-spermatozoid interactions (Quinn and Ackerman 2011). It is known that molluscan sperm cells are adapted to particular shear stress conditions (Zimmer and Riffell 2011). Conversely, the particular *C. gigas* timing, at the start of the ebbing of spring tides, reduces the time window during which spermatozoids and eggs interact prior to gamete dilution and decreases the efficiency of encounters. Concurrently, the time in which sperm attachment to an egg membrane must be completed is reduced as sperm and eggs are rapidly diluted to low concentrations. Thus, this timing favors the most rapid encounters and is clearly a form of selective pressure acting on both sexes (Levitan 2004; Bode and Marshall 2007). Importantly, this timing also reduces the risk of polyspermy (the fusion of more than one spermatozoan with an egg) and inviable embryos, which occur when the rate of sperm–egg collisions exceed the ability of the egg to block excess sperm. Polyspermy is considered a fundamental mechanism driving the evolution of speciation and reproduction in marine animals (Levitan et al. 2007; Gravilets 2014). In this context, the performance of *C. gigas* sperm, a low-speed sperm (straight line velocity ≈50 μm s^{-1}) active for up to 24 h (Suquet et al. 2012), is paramount. These characteristics can now be considered in light of the particular ecological situation described here, where spawning occurs in flow ranging from 0.4 m s^{-1} to 0.6 m s^{-1}. Another consequence of this timing is that the

release of eggs at early ebbing is a mechanism to minimize egg predation by dilution in large volumes and the acceleration of dispersal, although the dynamics of egg predation remain poorly understood. This concept has been thoroughly discussed for reef fish eggs (Claydon 2004) and crab eggs and larvae (Morgan and Christy 1995). During the oyster reproductive period, there are no fish larvae that feed on oyster larvae in the ecosystems studied. The potential predators could be planktivores in the water column during routine planktivorous activity and all benthic invertebrates that might filter eggs that pass over these organisms. Gametes can either be ingested or rejected as pseudofeces, but in either case, these organisms die (Morgan 1992). Moreover, a large number of gametes must sediment and integrate into the pool of organic matter, although the importance of the different fractions has not been investigated.

In conclusion, a delicate balance between the benefits and drawbacks of an appropriate high flow rate and turbulence exists at the beginning of ebbing for oysters. The physiological and ecological consequences are important, and spawning in the high waters of spring tides facilitates the spawning of as many oysters as possible in an ecosystem. This timing is likely to occur during an optimal situation in an intertidal ecosystem for fertilization success, recruitment and coverage of the entire surface with potential for colonization. However, species-specific strong differences occur for numerous broadcast spawners that spawn at low tide to minimize sperm dilution resulting from water motion (Yund 2000). The present report provides additional information on the timing and hydrodynamic conditions under which broadcast spawners can work in the field, but little is known about natural spawning in many taxa. Clearly, much more in situ information is needed to assess what flow regimes are associated with broadcast spawning in natural populations and successful fertilization.

References

Arakawa, K. Y. 1990. Natural spat collecting in the Pacific oyster *Crassostrea gigas* (Thunberg). Mar. Behav. Physiol. **17**: 95–128. doi:10.1080/10236249009378760

Baba, K., M. Tada, T. Kawajiri, and Y. Kuwara. 1999. Effects of temperature and salinity on spawning of the brackhish water bivalve *Corbicula japonica* in lake Abashiri, Japan. Mar. Ecol. Prog. Ser. **180**: 213–221. doi:10.3354/meps180213

Bentley, M. G., P. J. Olive, W. Last, and K. Jan. 2001. Sexual satellites, moonlight and the nuptial dances of worms: The influence of the moon on the reproduction of marine animals. Earth Moon Planets **85–86**: 67–84. doi:10.1023/A:1017039110161

Bernay, B., M. Baudy-Floc'h, B. Zanuttini, C. Zatylny, S. Pouvreau, and J. Henry. 2006. Ovarian and sperm regulatory peptides regulate ovulation in the oyster Crassostrea gigas. Mol. Reprod. Dev. **73**: 607–616. doi:10.1002/mrd.20472

Bode, M., and D. J. Marshall. 2007. The quick and the dead? Sperm competition and sexual conflict in sea. Evolution **61**: 2693–2700. doi:10.1111/j.1558-5646.2007.00232.x

Breese, W. P., and A. Robinson. 1981. Razor clams, *Siliqua patula* (Dixon): Gonadal development induced spawning and larval rearing. Aquaculture **22**: 27–33. doi:10.1016/0044-8486(81)90130-7

Caspers, H. 1984. Spawning periodicity and habitat of the palolo worm *Eunice viridis* (Polychaeta: Eunicidae) in the Samoan Islands. Mar. Biol. **79**: 229–236. doi:10.1007/BF00393254

Claydon, J. 2004. Spawning aggregations of coral reef fishes: Characteristics, hypotheses, threats and management. Ocean Mar. Biol. Ann. Rev. **42**: 265–302. doi:10.1080/02723646.2015.1023243

Claydon, J., M. I. McCormick, and G. P. Jones. 2014. Multi-species spawning sites for fishes on a low-latitude coral reef: Spatial and temporal patterns. J. Fish Biol. **84**: 1136–1163. doi:10.1111/jfb.12355

Denny, M. W., and M. Shibata. 1989. Consequences of surf-zone turbulence for settlement and fertilization. Am. Nat. **134**: 859–889. doi:10.1086/285018

Dupuy, J. L., N. T. Windsor, and C. E. Sutton. 1977. Manual for design and operation of an oyster seed hatchery for the American oyster, *Crassostrea virginica*. Special Report in Applied Marine Science and Ocean Engineering, 142. VIMS, Gloucester Point, Virginia.

Ellis, S. 1998. Spawning and early larval rearing of giant clams (Bivalvia: Tridacnidae). Cent. Trop. Subtrop. Aquac. Publ. **130**: 1–55.

Fournier, J., E. Levesque, S. Pouvreau, M. Le Pennec, and G. Le Moullac. 2012. Influence of plankton concentration on gametogenesis and spawning of the black lip pearl oyster Pinctada margaritifera in the Ahe lagoon (Tuamotu Archipelago, French Polynesia). Mar. Pollut. Bull. **65**: 463–470. doi:10.1016/j.marpolbul.2012.03.027

Fujiya, M. 1970. Oyster farming in Japan. Helgoländer wiss. Meeresunters **20**: 464–479. doi:10.1007/BF01609922

Galtsoff, P. S. 1930. The role of chemical stimulation in the spawning reaction of *Ostrea virginica*. Proc. Natl. Acad. Sci. USA **16**: 555–559. doi:10.1073/pnas.16.9.555

Galtsoff, P. S. 1938a. Physiology of reproduction of *Ostrea virginica*: I. Spawning reactions of the female and male. Biol. Bull. **74**: 461–486. doi:10.2307/1537816

Galtsoff, P. S. 1938b. Physiology of reproduction of *Ostrea virginica*: II. Stimulation of spawning in the female oyster. Biol. Bull. **75**: 286–307. doi:10.2307/1537736

Galtsoff, P. S. 1961. Physiology of reproduction in molluscs. Am. Zool. **1**: 273–289. http://dx.doi.org/10.1093/icb/1.2.273

Grangeré, K., A. Menesguen, S. Lefebvre, C. Bacher, and S. Pouvreau. 2009. Modelling the influence of environmental factors on the physiological status of the Pacific oyster *Crassostrea gigas* in an estuarine embayment; The Baie des

Veys (France). J. Sea Res. **62**: 147–158. doi:10.1016/j.seares.2009.02.002

Gravilets, S. 2014. Is sexual conflict an "Engine of speciation"? Cold Spring Harb. Perspect. Biol. **6**: a017723. doi:10.1101/cshperspect.a017723

Helm, M. M., N. Bourne, A. Lovatelli. (2004) Hatchery culture of bivalves. A practical manual. FAO Fisheries. Technical Paper. No. 471. Rome, FAO. 2004. 177 p.

Helmuth, B., C. D. G. Harley, P. M. Halpin, M. O'Donnell, G. E. Hofmann, and C. A. Blanchette. 2002. Climate change and latitudinal patterns of intertidal thermal stress. Science **298**: 1015–1017. doi:10.1126/science.1076814

Hendriks, I. E., L. A. Van Duren, and P. M. J. Herman. 2005. Image analysis techniques: A tool for the identification of bivalve larvae? J. Sea Res. **54**: 151–162. doi:10.1016/j.seares.2005.03.001

Henshaw, J. M., D. J. Marshall, M. D. Jennions, and H. Kokko. 2014. Local gamete competition explains sex allocation and fertilization strategies in the sea. Am. Nat. **184**: E32–E49. doi:10.1086/676641

His, E. 1976. Contribution à l'étude biologique de l'Huître dans le Bassin d'Arcachon, activité valvaire de *Crassostrea angulata* et de *Crassostrea gigas*; application à l'étude de la reproduction de l'Huître Japonaise. Ph.D. thesis. Université Bordeaux 1. http://archimer.ifremer.fr/doc/1976/these-3352.pdf

Hopkins, A. E. 1936. Ecological observations on spawning and early larval development in the olympia oyster (*Ostrea Lurida*). Ecology **17**: 551–566. doi:10.2307/1932760

Korringa, P. 1947. Relations between the moon and periodicity in the breeding of marine animals. Ecol. Monogr. **17**: 347–381. http://dx.doi.org/10.2307/1948665

Lamare, M. D., and B. G. Stewart. 1998. Mass spawning by the sea urchin *Evechinus chloroticus* (Echinodermata: Echinoidea) in a New Zealand fiord. Mar. Biol. **132**: 135–140. doi:10.1007/s002270050379

Levitan, D. R. 2004. Density-dependent sexual selection in external fertilizers: Variances in male and female fertilization success along the continuum from sperm limitation to sexual conflict in the sea urchin *Strongylocentrotus franciscanus*. Am. Nat. **164**: 298–309. doi:10.1086/423150

Levitan, D. R., and C. Petersen. 1995. Sperm limitation in the sea. Trends Ecol. Evol. **10**: 228–231. doi:10.1016/S0169-5347(00)89071-0

Levitan, D. R., C. TerHorst, and N. Fogarty. 2007. The risk of polyspermy in three congeneric sea urchins ad its implications for gametic incompatibility and reproductive isolation. Evolution **61**: 2009–2016. doi:10.1111/j.1558-5646.2007.00150.x

Loosanoff, V. L., and C. A. Nomejko. 1951. Spawning and setting of the American oyster, *O. virginica*, in relation to lunar phases. Ecology **32**: 113–134. http://dx.doi.org/10.2307/1930976

Loosanoff, V. L., H. C. Davis, and P. E. Chanley. 1966. Dimensions and shapes of larvae of some marine bivalve mollusks. Malacologia **4**: 351–435. https://archive.org/details/cbarchive_48893_dimensionsandshapesoflarvaeofs1966

Marshall, D. J. 2002. In situ measures of spawning synchrony and fertilization success in an intertidal, free-spawning invertebrate. Mar. Ecol. Prog. Ser. **236**: 113–119. doi:10.3354/meps236113

Marshall, D. J., D. Semmens, and C. Cook. 2004. Consequences of spawning at low tide: Limited gamete dispersal for a rockpool anemone. Mar. Ecol. Prog. Ser. **266**: 135–142. doi:10.3354/meps266135

Matias, D., S. Joaquim, A. Leitao, and C. Massapina. 2009. Effect of geographic origin, temperature and timing of broodstock collection on conditioning, spawning success and larval viability of *Ruditapes decussatus* (Linné, 1758). Aquac. Int. **17**: 257–271. doi:10.1007/s10499-008-9197-3

Mercier, A., R. H. Ycaza, and J.-F. Hamel. 2007. Long-term study of gamete release in a broadcast-spawning holothurian: Predictable lunar and diel periodicities. Mar. Ecol. Prog. Ser. **329**: 179–189. doi:10.3354/meps329179

Minchin, D. 1992. Multiple species, mass spawning events in an Irish sea Lough: The effect of temperatures on spawning and recruitment of invertebrates. Invertebr. Reprod. Dev. **22**: 229–238. doi:10.1080/07924259.1992.9672275

Morgan, S. G. 1992. Predation by planktonic and benthic invertebrates on larvae of estuarine crabs. J. Exp. Mar. Biol. Ecol. **163**: 91–110. doi:10.1016/0022-0981(92)90149-5

Morgan, S. G., and J. H. Christy. 1995. Adaptive significance of the timing of larval release by crabs. Am. Nat. **145**: 457–479. doi:10.1086/285749

Nelson, T. C. 1928. Relation of spawning of the oyster to temperature. Ecology **9**: 145–154. doi:10.2307/1929351

Pearson, G. A., E. A. Serrão, and S. H. Brawley. 1998. Control of gamete release in fucoid algae: Sensing hydrodynamic conditions via carbon acquisition. Ecology **79**: 1725–1739. doi:10.2307/176791

Pouvreau, S., M. Rambeau, J. C. Cochard, and R. Robert. 2006. Investigation of marine bivalve morphology by RMN imaging: First anatomical results of a promising technique. Aquaculture **259**: 415–423. doi:10.1016/j.aquaculture.2006.05.018

Pronker, A. E., N. M. Nevejan, F. Peene, P. Geijsen, and P. Sorgeloos. 2008. Hatchery broodstock conditioning of the blue mussel *Mytilus edulis* (Linnaeus 1758): Part I. Impact of different micro-algae mixtures on broodstock performance. Aquac. Int. **16**: 297–307. doi:10.1007/s10499-007-9143-9

Prytherch, H. F. 1929. Investigation of the physical conditions controlling spawning of oysters and the occurrence, distribution, and setting of oyster larvae in Milford Harbor, Connecticut. Bull. US Bttr. Fisll. **44**: 429–503.

Quinn, N. P., and J. D. Ackerman. 2011. The effect of near-bed turbulence on sperm dilution and fertilization success

of broadcast-spawning bivalves. Limnol. Oceanogr. **1**: 176–193. doi:10.1215/21573698-1504517

Quinn, N. P., and J. D. Ackerman. 2012. Biological and ecological mechanisms for overcoming sperm limitation in dreissenid mussels. Aquat. Sci. **74**: 415–425. doi:10.1007/s00027-011-0237-0

R Development Core Team. 2011. R: A Language and Environment for Statistical Computing. R Foundation for Statistical Computing, Vienna, Austria, ISBN 3-900051-07-0.

Rice, P., S. Ray, S. Painter, and G. Nagle. 2002. An intrinsic membrane protein in oyster sperm stimulates spawning behaviors in *Crassostrea virginica*: Implications for aquaculture. J. Shellfish Res. **21**: 715–718.

Royer, J., C. Seguineau, K.-I. Park, S. Pouvreau, K.-S. Choi, and K. Costil. 2008. Gametogenetic cycle and reproductive effort assessed by two methods in 3 age classes of Pacific oysters, *Crassostrea gigas*, reared in Normandy. Aquaculture **277**: 313–320. doi:10.1016/j.aquaculture.2008.02.033

Schwartzmann, C., G. Durrieu, M. Sow, P. Ciret, C. E. Lazareth, and J.-C. Massabuau. 2011. In situ giant clam growth rate behavior in relation to temperature: A one year coupled study of high-frequency non-invasive valvometry and sclerochronology. Limnol. Oceanogr. **56**: 1940–1951. doi:10.4319/lo.2011.56.5.1940

Serrão, E. A., and J. Havenhand. 2009. Fertilization strategies, p. 149–164. *In* M. Wahl [ed.], Marine hard bottom communities, v. 206. Ecological Studies. Springer-Verlag Berlin Heidelberg. doi:10.1007/978-3-540-92704-4_10

Southgate, P. C., and A. C. Beer. 1997. Hatchery and early nursery culture of the blacklip pearl oyster (*Pinctada margaritifera*, L.). J. Shellfish Res. **16**: 561–567. http://ia600509.us.archive.org/14/items/journalofshellfi16nati/journalofshellfi16nati.pdf

Southgate, P. C., and P. S. Lee. 1998. Hatchery rearing of the tropical blacklip oyster *Saccostrea echinata* (Quoy and Gaimard). Aquaculture **169**: 275–281. doi:10.1016/S0044-8486(98)00382-2

Sow, M., G. Durrieu, L. Briollais, P. Ciret, and J.-C. Massabuau. 2011. Water quality assessment by means of valvometry and high-frequency data modeling. Environ. Monit. Assess. **182**: 155–170. doi:10.1007/s10661-010-1866-9

Starr, M., J. Himmelman, and J. Therriault. 1990. Direct coupling of marine invertebrate spawning with phytoplankton blooms. Science **247**: 1071. doi:10.1126/science.247.4946.1071

Suquet, M., and others. 2012. Marathon vs sprint racers: An adaptation of sperm characteristics to the reproductive strategy of Pacific oyster, turbot and seabass. J. Appl. Ichthyol. **28**: 956–960. doi:10.1111/jai.12061

Sweeney, A. M., C. A., Boch, S. Johnsen, and D. E. Morse. 2011. Twilight spectral dynamics and the coral reef invertebrate spawning response. J. Exp. Biol. **214**: 770–777. doi:10.1242/jeb.043406

Tran, D., P. Ciret, A. Ciutat, G. Durrieu, and J.-C. Massabuau. 2003. Estimation of potential and limits of bivalve closure response to detect contaminants: Application to cadmium. Environ. Toxicol. Chem. **22**: 914–920. doi:10.1002/etc.5620220432

Tran, D., J.-C. Massabuau, and C. Vercelli. 2008. Influence of sex and spawning status on blood oxygenation status in oysters *Crassostrea gigas* in a Mediterranean lagoon (Thau, France). Aquaculture **277**: 58–65. doi:10.1016/j.aquaculture.2008.02.002

Tran, D., A. Nadau, G. Durrieu, P. Ciret, J.-P. Parisot, and J.-C. Massabuau. 2011. Field chronobiology in a molluscan bivalve: How the moon and sun cycles interact to drive oyster activity rhythms. Chronobiol. Int. **28**: 307–317. doi:10.3109/07420528.2011.565897

Watson, G. J., M. E. Williams, and M. G. Bentley. 2000. Can synchronous spawning be predicted from environmental parameters? A case study of the lugworm *Arenicola marina*. Mar. Biol. **136**: 1003–1017. doi:10.1007/s002270000283

Yund, P. O. 2000. How severe is sperm limitation in natural populations of marine free-spawners? Trends Ecol. Evol. **15**: 10–13. http://dx.doi.org/10.1016/S0169-5347(99)01744-9

Zimmer, R. K., and J. A. Riffell. 2011. Sperm chemotaxis, fluid shear, and the evolution of sexual reproduction. Proc. Natl. Acad. Sci. **108**: 13200–13205. doi:10.1073/pnas.1018666108

Acknowledgments

The authors would like to thank the personnel from Ifremer LER, particularly S. Guesdon and J.-L. Seugnet, and from UMR CNRS 5805 EPOC, Stéphane Bujan, Thierry Corrège, Henri Bouillard, Christian Portier and Bruno Etcheverria. This work involved the use of larvae data from Arcachon Bay, collected by generations of scientists at Ifremer. The authors would like to thank two anonymous reviewers for the insightful comments on a previous draft of this manuscript. This work was funded by a grant from the CNRS (Centre National de la Recherche Scientifique), the University of Bordeaux, the Région Aquitaine, France, OSQUAR program and the MolluSCAN eye Project. I. Bernard and S. Pouvreau were funded by the VeLyGer project (www.ifremer.fr/velyger), French Ministry of Agriculture (DPMA), European Community (FEP) and Ifremer (conv. no. 30 114-2008). I. Bernard was supported by a scholarship provided by Ifremer and the Conseil Regional de Poitou-Charentes (France).

Submitted 9 March 2015
Revised 23 June 2015; 21 October 2015
Accepted 4 November 2015

Associate editor: Josef Ackerman